
Since January 2020 Elsevier has created a COVID-19 resource centre with free information in English and Mandarin on the novel coronavirus COVID-19. The COVID-19 resource centre is hosted on Elsevier Connect, the company's public news and information website.

Archivos de Bronconeumología 58(S1) (2022) 69–72

Sociedad Española de Neumología y Cirugía Torácica SEPAR

ARCHIVOS DE Bronconeumología

www.archbronconeumol.org

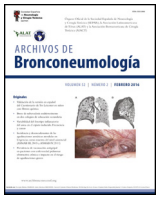

Scientific Letter

## Chest CT as a Prognostic Tool in COVID-19

### *La TC de tórax como herramienta pronóstica en COVID-19*

*To the Director,*

Considering the high variability of clinical course in the COVID-19, prognostic tools remain necessary for strategic healthcare planning. In hospitalized patients, clinical and demographic characteristics are associated with greater complications and death due to the disease.[1–4] Chest computed tomography (CT) has also been widely used in the evaluation of these patients due to its high sensitivity,[5] speed and relative availability, not only as a complementary diagnostic tool but also as an auxiliary method in clinical management and risk stratification.[6,7] Therefore, the objective of our study is to analyze tomographic findings at admission of hospitalized patients with COVID-19 and their relationship with disease severity, using the need for invasive mechanical ventilation (MV) and in-hospital mortality as main outcomes.

We conducted a cross-sectional analysis of all confirmed COVID-19 cases in hospitalized adult patients, from January through December 2020, at a tertiary care public university referral hospital for COVID-19 care in Curitiba, the largest city in southern Brazil. We excluded patients who did not undergo chest CT or whose chest CT was performed outside the period of 5 days after hospital admission, as well as patients with incomplete data.

Chest CT was performed with high-resolution technique, with patients in a supine position and in complete inspiration, on a Toshiba Aquilion 64 CT scanner. The images were evaluated by certified radiologists. Patients were evaluated regarding the predominant tomographic pattern, which was considered to affect more than 50% of involved lung parenchyma. Patterns considered were ground-glass opacities, crazy paving (ground-glass opacities with intralobular septal thickening), consolidation and mixed pattern (half of the affected area with consolidation and the remainder with another tomographic pattern). Pulmonary artery diameter (PAD) and the dimensions of the mediastinal lymph nodes were evaluated in axial plane. Lymph nodes were considered enlarged when the smallest diameter found was greater than 10 mm. The extent of lung parenchyma involvement was estimated according to visual scale in the axial plane and categorized into none, less than 25%, 25–50%, 50–75% and more than 75%. Clinical, laboratory, and demographic data were also collected.

Statistical analysis was performed using IBM SPSS Statistics software version 27. Quantitative variables were described in means ± standard deviation or median (interquartile range [IQR]), as appropriate. Categorical variables were described as frequencies and percentages. The relationship of demographic, clinical and tomographic variables with mortality and the need for MV was evaluated using univariate logistic regression. A multivariate logistic regression was further performed to identify independent predictors. Only variables with at least 690 valid entries and with $p$ values <0.05 in the univariate logistic regression analysis were included. The stepwise backward approach was used. Odds ratio (OR) with a 95% confidence interval (CI) were reported for all the variables analyzed. $P$ values <0.05 were considered statistically significant.

In 2020, 1246 patients were hospitalized due to COVID-19 in our hospital, 492 of which were excluded from our analysis (Supplementary Fig. 1); thus, we assessed 754 patients. The mean age was 56.3 ± 14.7 years old. The median time of symptoms onset until admission was 8 days (IQR 6–11). Clinical and demographic characteristics of the study population are shown in Supplementary Table 1.

Chest CT was performed within the first two days of hospitalization (median 0, IQR 0–1) in 86.7% of patients, with a median time between onset of symptoms and chest CT of 9 days (IQR 6–11). Similarly to data already reported,[7–9] the most frequent finding was ground-glass opacity (53.9%), related to pulmonary alveolar oedema and partial filling of alveoli by proteinaceous exudate in the early stages of the disease[10–12] (Table 1). As the disease progresses, with lymphocyte activation and release of inflammatory cytokines, these changes may become more extensive and there may be intra and interlobular septal infiltration with the presence of crazy paving, indicating both alveolar and interstitial involvement due to COVID-19.[12,13] This pathophysiological mechanism seems to be related to the clinical worsening, which is in line with our findings, where crazy paving was found in 10.7% of our cases and, although not statistically significant regarding mortality in this analysis, was associated with more severe disease when compared to ground-glass opacities. Table 2 and Supplementary Table 2 show the characteristics of patients who died or needed MV, in comparison with those who did not.

When assessing the extent of lung disease on chest CT, half of the patients had parenchyma involvement greater than 50%. Greater lung parenchyma involvement was significantly associated with high values of CRP, ferritin and LDH and low lymphocytes and albumin, probably indicating that these findings are related to more extensive involvement on CT. In addition, lung parenchyma involvement greater than 75% was independently associated with a higher risk of clinical worsening (OR = 2.25, 95% CI 1.39–3.63, $p < 0.001$) and death (OR = 2.6, 95% CI 1.37–3.09, $p < 0.001$). The relationship between the degree of lung parenchyma involvement, assessed by different scores, and worse outcomes for COVID-19 has also been described in other studies,[8,9,11,14] which reinforces the role of chest CT as a prognostic tool for COVID-19.

Another independent predictor of mortality identified in chest CT was the presence of pleural effusion, found in 11.5% of patients,

https://doi.org/10.1016/j.arbres.2022.02.006

**Table 1**
Chest computed tomography results.

| Chest CT characteristics | | | | | |
|---|---|---|---|---|---|
| Dominant pattern | *N* = 736 | Lung involvement | *N* = 749 | Other findings | *N* = 754 |
| Ground-glass opacity | 397 (53.9%) | None | 12 (1.6%) | Pleural effusion | 87 (11.5%) |
| Consolidation | 53 (7.2%) | <25% | 122 (16.3%) | Lymph node enlargement | 158 (21.0%) |
| Crazy paving | 81 (11%) | 25–50% | 239 (31.9%) | PAD[a] (mm) | 27.6 ± 4.2 |
| Mixed | 205 (27.9%) | 50–75% | 215 (28.7%) | PAD > 30 mm | 167 (22.1%) |
| | | >75% | 161 (21.5%) | | |
| | Laboratory abnormalities according to the degree of lung involvement in chest CT | | | | |
| | <25% | 25–50% | 50–75% | >75% | *p*[*] |
| Lymphocytes[b] | 134, 1152 (738–1766) | 238, 881 (565–1304) | 215, 850 (531–1200) | 161, 765 (533–1065) | <0.001 |
| D-Dimer[b] | 121, 1.12 (0.52–4.05) | 217, 0.77 (0.45–1.44) | 207, 0.95 (0.54–1.79) | 157, 0.96 (0.6–2.09) | 0.009 |
| Albumin[c] | 113, 3.63 ± 0.59 | 193, 3.63 ± 0.47 | 174, 3.57 ± 0.44 | 137, 3.37 ± 0.45 | <0.001 |
| LDH[b] | 110, 269 (7–334) | 18, 333 (62–416) | 181, 384 (96–492) | 143, 420 (330–591) | <0.001 |
| Ferritin[b] | 105, 453 (168–989) | 193, 830 (26–1527) | 189, 1144 (439–1675) | 159, 1547 (836–1675) | <0.001 |
| C-reactive protein[b] | 128, 2.54 (0.88–7.27) | 232, 6.06 (2.99–11.63) | 212, 7.86 (4.9–13.92) | 161, 12.36 (6.83–16) | <0.001 |
| Procalcitonin[b] | 24, 0.13 (0.04–1.02) | 45, 0.1 (0.05–0.55) | 53, 0.11 (0.05–0.54) | 55, 0.15 (0.08–0.45) | 0.463 |
| | Pairwise comparison analysis of laboratory abnormalities according to the degree of lung involvement in chest CT | | | | |
| | Lymphocytes[d] | Albumin[d] | C-reactive protein[d] | Ferritin[d] | LDH[d] |
| <25% vs. 25-50% | <0.001 | 1 | <0.001 | 0.003 | 0.029 |
| <25% vs. 50-75% | <0.001 | 1 | <0.001 | <0.001 | <0.001 |
| <25% vs. >75% | <0.001 | <0.001 | <0.001 | <0.001 | <0.001 |
| 25–50% vs. 50–75% | 0.547 | 1 | 0.045 | 0.305 | 0.003 |
| 25−−50% vs. >75% | 0.036 | <0.001 | <0.001 | <0.001 | <0.001 |
| 50–75% vs. >75% | 1 | 0.001 | 0.001 | 0.003 | 0.054 |
| | Relationship between pulmonary artery diameter (PAD) and laboratory abnormalities according to reference values | | | | |
| | Value (n) | PAD (mm)[a] | Value (*n*) | PAD (mm)[a] | *P*[#] |
| Lymphocytes (×10³/μL) | ≥1000 (317) | 27.2 ± 4.1 | <1000 (436) | 27.8 ± 4.3 | 0.065 |
| D-Dimer (mg/L FEU) | ≤0.55 (199) | 27.1 ± 4.1 | >0.55 (507) | 27.9 ± 4.3 | 0.023 |
| Albumin (g/dL) | ≥3.5 (396) | 27.2 ± 4.0 | <3.5 (225) | 28.3 ± 4.5 | 0.001 |
| Cardiac troponin (pg/ml) | <15.6 (435) | 27.1 ± 3.8 | ≥15.6 (135) | 29.7 ± 4.7 | <0.001 |
| LDH (U/L) | <220 (61) | 27.2 ± 3.1 | ≥220 (567) | 27.7 ± 4.3 | 0.305 |
| Ferritin (ng/mL) | ≤204 (74) | 27.9 ± 4.5 | >204 (567) | 27.6 ± 4.2 | 0.562 |
| C-reactive protein (mg/dL) | ≤0.5 (28) | 27.6 ± 3.6 | >0.5 (710) | 27.5 ± 4.2 | 0.92 |
| Procalcitonin (ng/mL) | <0.5 (132) | 27.4 ± 4.3 | ≥0.5 (45) | 27.9 ± 3.9 | 0.544 |

PAD: pulmonary artery diameter.
Data reported in *n* (%), except when indicated otherwise.
[a] Mean ± standard deviation.
[b] *n*, median (IQR).
[c] *n*, mean ± standard deviation.
[d] One way ANOVA and Bonferroni Test, $p < 0.05$.
[*] One way ANOVA (leukocytes, lymphocytes, albumin, LDH, ferritin, C-reactive protein); Kruskal–Wallis (d-dimer, procalcitonin); $p < 0.05$.
[#] Student's t-test for independent samples, $p < 0.05$.

with an adjusted OR of 2.36 (95% CI 1.33–4.19, $p = 0.003$) compared to patients without it. A similar result was found in a meta-analysis which reported a 9.5% prevalence of pleural effusion, with an OR of 4.53 (95% CI 2.16–9.49) for mortality in this group.[15] This fact seems to be associated with direct injury to the lung tissue by SARS-CoV-2 and with a higher systemic inflammatory response,[16] analogous to that already described in other viral respiratory infections, such as MERS[17] and H1N1.[18]

In our cohort, patients who needed MV or who died from COVID-19 also had larger PAD. The mean PAD was 27.6 ± 4.2 mm and a diameter greater than 30 mm was found in 167 patients (22.1%). Esposito et al. reported a relationship between PAD enlargement and in-hospital mortality due to COVID-19, even after adjustment for demographic characteristics and comorbidities, suggesting that this is an acute complication of the disease.[19] The main mechanism related to larger PAD is related to increased pulmonary vascular resistance, secondary to endothelial injury, tissue inflammation and prothrombotic state with occlusion of small vessels.[20] Although cardiovascular and thromboembolic complications were not evaluated in this study, patients with higher D-dimer and cardiac troponin presented significantly larger PAD when compared to patients with normal values (27.1 ± 4.1 mm vs. 27.9 ± 4.3, $p = 0.023$; and 27.1 ± 3.8 vs. 29.7 ± 4.7, $p < 0.001$, respectively).

This study has limitations. The collection of data from medical records led to the exclusion of patients due to incomplete data since care was provided without a standardized protocol of data collection. Another limitation is that all patients were admitted to the same public hospital, so data may not accurately represent the reality of other regions.

In conclusion, easily obtainable chest CT data, such as extent of lung involvement in visual scale, PAD and presence of pleural effusion, can be used as predictors of disease severity and in-hospital mortality in COVID-19.

## Ethics approval

The study was previously approved by the local Research Ethics Committee, under the opinion 4.215.032, of August 16th, 2020, with waiver of informed consent.

**Table 2**
Factors associated with in-hospital death.

| Clinical characteristics | *N* | Hospital Discharge | Death | OR | CI95% | *p*[*] |
|---|---|---|---|---|---|---|
| Age ≥ 60 years old | 318 | 224 (70.4%) | 94 (29.6%) | 4.66 | 3.07–7.08 | <0.001 |
| Male sex | 390 | 325 (83.3%) | 65 (16.7%) | 0.92 | 0.63–1.34 | 0.665 |
| Smoking history | 177 | 134 (75.7%) | 43 (24.3%) | 2.15 | 1.36–3.39 | 0.001 |
| Obesity | 224 | 194 (86.6%) | 30 (13.4%) | 0.66 | 0.43–1.03 | 0.07 |
| Hypertension | 379 | 305 (80.5%) | 74 (19.5%) | 1.38 | 0.94–2.02 | 0.096 |
| Diabetes Mellitus | 238 | 190 (79.8%) | 48 (20.2%) | 1.34 | 0.90–1.98 | 0.149 |
| Coronary artery disease | 63 | 49 (77.8%) | 12 (22.2%) | 1.42 | 0.76–2.65 | 0.276 |
| COPD | 48 | 34 (70.8%) | 14 (29.2%) | 2.09 | 1.09–4.03 | 0.027 |
| Chronic heart disease | 132 | 101 (76.5%) | 31 (23.5%) | 1.62 | 1.03–2.56 | 0.038 |
| Chronic lung disease | 110 | 85 (77.3%) | 25 (22.7%) | 1.51 | 0.92–2.47 | 0.101 |
| Chronic liver disease | 8 | 3 (37.5%) | 5 (62.5%) | 8.28 | 1.95–35.1 | 0.004 |
| Chronic kidney disease | 34 | 21 (61.8%) | 13 (38.2%) | 3.19 | 1.55–6.55 | 0.002 |
| Active cancer | 33 | 21 (63.6%) | 12 (36.4%) | 2.92 | 1.40–6.10 | 0.004 |
| **Laboratory tests** | ***N*** | **Hospital discharge** | **Death** | **OR** | **95% CI** | ***p*[*]** |
| Lymphocytes[a,b] | 753 | 623, 910 (577–1327) | 130, 760 (462–1013) | 0.92 | 0.89–0.96 | <0.001 |
| C-reactive protein[b] | 738 | 608, 6.58 (2.91–12.68) | 130, 10.52 (5.54–15.62) | 1.08 | 1.04–1.12 | <0.001 |
| Ferritin[a,b] | 641 | 520, 900 (412–1675) | 121, 1210 (478–1675) | 1.04 | 1.003–1.07 | 0.031 |
| LDH[a,b] | 628 | 511, 336 (263–428) | 117, 436 (319–593) | 1.4 | 1.26–1.55 | <0.001 |
| D-Dimer[b] | 706 | 581, 0.84 (0.48–1.71) | 125, 1.44 (0.77–3.67) | 1.03 | 1.01–1.05 | 0.009 |
| Albumin[c] | 621 | 507, 3.61 ± 0.45 | 114, 3.32 ± 0.60 | 0.32 | 0.21–0.49 | <0.001 |
| Procalcitonin[b] | 177 | 104, 0.09 (0.05–0.24) | 73, 0.26 (0.08–1.35) | 1.27 | 1.01–1.59 | 0.039 |
| Cardiac troponin[a,b] | 570 | 455, 10 (10–10) | 115, 14.3 (10–61.40) | 1.01 | 0.99–1.03 | 0.394 |
| **Chest CT** | ***N*** | **Hospital discharge** | **Death** | **OR** | **95% CI** | ***p*[*]** |
| *Lung involvement area* | | | | | | |
| ≤75%[d] | 588 | 505 (85.9%) | 83 (14.1%) | | | |
| >75% | 161 | 114 (70.8%) | 47 (29.2%) | 2.51 | 1.66–3.78 | <0.001 |
| *Dominant pattern* | | | | | | |
| Ground-glass opacity[d] | 397 | 323 (81.4%) | 74 (18.6%) | | | |
| Mixed | 205 | 181 (88.3%) | 24 (11.7%) | 0.58 | 0.35–0.95 | 0.03 |
| Crazy paving | 81 | 59 (72.8%) | 22 (27.2%) | 1.63 | 0.94–2.82 | 0.083 |
| Consolidation | 53 | 45 (84.9%) | 8 (15.1%) | 0.78 | 0.35–1.72 | 0.531 |
| Pleural effusion | 87 | 56 (64.4%) | 31 (35.6%) | 3.18 | 1.95–5.17 | <0.001 |
| *Lymph node enlargement* | 158 | 120 (76.0%) | 38 (24.1%) | 1.73 | 1.13–2.66 | 0.011 |
| *PAD (mm)*[c] | 754 | 624, 27.3 ± 4.1 | 139, 28.9 ± 4.6 | 1.09 | 1.04–1.13 | <0.001 |
| | | Independent predictors of in-hospital mortality (multivariate analysis)[e] | | | | |
| | | OR | 95% CI | *p*[*] | | |
| Age ≥ 60 years old | | 4.38 | 2.76–6.95 | <0.001 | | |
| Active cancer | | 2.99 | 1.21–7.17 | 0.018 | | |
| Chronic liver disease | | 11.58 | 2.22–60.38 | 0.004 | | |
| Lymphocytes[a] | | 0.95 | 0.91–0.997 | 0.037 | | |
| C-reactive protein | | 1.05 | 1.002–1.09 | 0.038 | | |
| Lung involvement > 75% | | 2.25 | 1.39–3.63 | <0.001 | | |
| Pleural effusion | | 2.36 | 1.33–4.19 | 0.003 | | |

[*] Logistic regression model and Wald test, $p < 0.05$.
[a] OR corresponds to each increment of 100 units of the variable.
[b] *n*, median (IQR).
[c] *n*, mean ± standard deviation.
[d] Reference variable.
[e] Variables initially included in the model: age ≥ 60 years old, chronic heart disease, chronic obstructive pulmonary disease, active cancer, chronic kidney disease, chronic liver disease, C-reactive protein, lymphocytes, D-dimer, lung parenchyma involvement >75%, pleural effusion and pulmonary artery diameter.

## Funding

This research did not receive any specific grant from funding agencies in the public, commercial, or not-for-profit sectors.

## Data availability statement

The datasets generated and analyzed during the current study are available from the corresponding author on reasonable request.

## Conflict of interest

None declared.

## Acknowledgements

The authors would like to thank all professionals involved in the care of patients with COVID-19, as well as patients themselves and their families.

## Appendix A. Supplementary data

Supplementary data associated with this article can be found, in the online version, at doi:10.1016/j.arbres.2022.02.006.

## References


1. Borobia A, Carcas A, Arnalich F, Álvarez-Sala R, Monserrat-Villatoro J, Quintana M, et al. A cohort of patients with COVID-19 in a major teaching hospital in Europe. JCM. 2020;9:1733, http://dx.doi.org/10.3390/jcm9061733.
2. Berenguer J, Ryan P, Rodríguez-Baño J, Jarrín I, Carratalà J, Pachón J, et al. Characteristics and predictors of death among 4035 consecutively hospitalized patients with COVID-19 in Spain. Clin Microbiol Infect. 2020;26:1525–36, http://dx.doi.org/10.1016/j.cmi.2020.07.024.
3. Marcolino MS, Ziegelmann PK, Souza-Silva MVR, Nascimento IJB, Oliveira LM, Monteiro LS, et al. Clinical characteristics and outcomes of patients hospitalized with COVID-19 in Brazil: results from the Brazilian COVID-19 registry. Int J Infect Dis. 2021;107:300–10, http://dx.doi.org/10.1016/j.ijid.2021.01.019.
4. Suleyman G, Fadel RA, Malette KM, Hammond C, Abdulla H, Entz A, et al. Clinical characteristics and morbidity associated with coronavirus disease 2019 in a series of patients in Metropolitan Detroit. JAMA Netw Open. 2020;3:e2012270, http://dx.doi.org/10.1001/jamanetworkopen.2020.12270.
5. Ai T, Yang Z, Hou H, Zhan C, Chen C, Lv W, et al. Correlation of chest CT and RT-PCR testing for coronavirus disease 2019 (COVID-19) in China: a report of 1014 cases. Radiology. 2020;296:E32–40, http://dx.doi.org/10.1148/radiol.2020200642.
6. Akl EA, Blažić I, Yaacoub S, Frija G, Chou R, Appiah JA, et al. Use of chest imaging in the diagnosis and management of COVID-19: a WHO rapid advice guide. Radiology. 2021;298:E63–9, http://dx.doi.org/10.1148/radiol.2020203173.
7. Yuan M, Yin W, Tao Z, Tan W, Hu Y. Association of radiologic findings with mortality of patients infected with 2019 novel coronavirus in Wuhan, China. PLOS ONE. 2020;15:e0230548, http://dx.doi.org/10.1371/journal.pone.0230548.
8. Mogami R, Lopes AJ, Araújo Filho RC, de Almeida FCS, Messeder A.M.D.C., Koifman A.C.B., et al. Chest computed tomography in COVID-19 pneumonia: a retrospective study of 155 patients at a university hospital in Rio de Janeiro, Brazil. Radiol Bras. 2021;54:1–8, http://dx.doi.org/10.1590/0100-3984.2020.0133.
9. Metwally MI, Basha MAA, Zaitoun MMA, Abdalla HM, Nofal HAE, Hendawy H, et al. Clinical and radiological imaging as prognostic predictors in COVID-19 patients. Egypt J Radiol Nucl Med. 2021;52:100, http://dx.doi.org/10.1186/s43055-021-00470-9.
10. Pan F, Ye T, Sun P, Gui S, Liang B, Li L, et al. Time course of lung changes at chest CT during recovery from coronavirus disease 2019 (COVID-19). Radiology. 2020;295:715–21, http://dx.doi.org/10.1148/radiol.2020200370.
11. Pan F, Zheng C, Ye T, Li L, Liu D, Li L, et al. Different computed tomography patterns of Coronavirus Disease 2019 (COVID-19) between survivors and non-survivors. Sci Rep. 2020;10:11336, http://dx.doi.org/10.1038/s41598-020-68057-4.
12. Tian S, Hu W, Niu L, Liu H, Xu H, Xiao SY. Pulmonary pathology of early-phase 2019 novel coronavirus (COVID-19) pneumonia in two patients with lung cancer. J Thorac Oncol. 2020;15:700–4, http://dx.doi.org/10.1016/j.jtho.2020.02.010.
13. Hansell DM, Bankier AA, MacMahon H, McLoud TC, Müller NL, Remy J. Fleischner Society: glossary of terms for thoracic imaging. Radiology. 2008;246:697–722, http://dx.doi.org/10.1148/radiol.2462070712.
14. Salvatore C, Roberta F, Angela L, Cesare P, Alfredo C, Giuliano G, et al. Clinical and laboratory data, radiological structured report findings and quantitative evaluation of lung involvement on baseline chest CT in COVID-19 patients to predict prognosis. Radiol Med. 2021;126:29–39, http://dx.doi.org/10.1007/s11547-020-01293-w.
15. Rathore SS, Hussain N, Manju AH, Wen Q, Tousif S, Avendaño-Capriles CA, et al. Prevalence and clinical outcomes of pleural effusion in COVID-19 patients: a systematic review and meta-analysis. J Med Virol. 2022;94:229–39, http://dx.doi.org/10.1002/jmv.27301.
16. Wei X, Wang X, Ye L, Niu Y, Peng W, Wang Z, et al. Pleural effusion as an indicator for the poor prognosis of COVID-19 patients. Int J Clin Pract. 2021;75, http://dx.doi.org/10.1111/ijcp.14123.
17. Das KM, Lee EY, Enani MA, AlJawder SE, Singh R, Bashir S, et al. CT correlation with outcomes in 15 patients with acute middle east respiratory syndrome coronavirus. Am J Roentgenol. 2015;204:736–42, http://dx.doi.org/10.2214/AJR.14.13671.
18. Schoen K, Horvat N, Guerreiro NFC, de Castro I, de Giassi KS. Spectrum of clinical and radiographic findings in patients with diagnosis of H1N1 and correlation with clinical severity. BMC Infect Dis. 2019;19:964, http://dx.doi.org/10.1186/s12879-019-4592-0.
19. Esposito A, Palmisano A, Toselli M, Vignale D, Cereda A, Rancoita PMV, et al. Chest CT-derived pulmonary artery enlargement at the admission predicts overall survival in COVID-19 patients: insight from 1461 consecutive patients in Italy. Eur Radiol. 2021;31:4031–41, http://dx.doi.org/10.1007/s00330-020-07622-x.
20. Varga Z, Flammer AJ, Steiger P, Haberecker M, Andermatt R, Zinkernagel AS, et al. Endothelial cell infection and endotheliitis in COVID-19. Lancet. 2020;395:1417–8, http://dx.doi.org/10.1016/S0140-6736(20)30937-5.



Mariane Gonçalves Martynychen Canan[a,*], Caroline Souza Sokoloski[a], Vitor Loureiro Dias[a], João Mario Clementin de Andrade[b], Ana Carolina Nicoletti Basso[b], Carolina Chomiski[b], Dante Luiz Escuissato[c], Itsem Campos Andrade Junior[d], Izabele Cristine Vaz[d], Rebecca Saray Marchesini Stival[e], Karin Mueller Storrer[f]

[a] *Cardio-Pulmonology Division, Federal University of Paraná, Curitiba, Brazil*
[b] *Federal University of Paraná, Curitiba, Brazil*
[c] *Radiology Unit, Federal University of Paraná, Curitiba, Brazil*
[d] *Medical School, Federal University of Paraná, Curitiba, Brazil*
[e] *Emergency Department, Federal University of Paraná, Curitiba, Brazil*
[f] *Department of Internal Medicine, Federal University of Paraná, Curitiba, Brazil*

Corresponding author.
*E-mail address:* mariane.canan@hc.ufpr.br (M.G.M. Canan).